DEVELOPMENT ON THE MICROPILE FOR APPLYING TO ARTIFICIAL GROUND ABOVE RAILROAD SITE

Young-Eun Jang[1], Jin-tae Han[2], Changho Choi[3]

ABSTRACT

The Korean government recently launched a new policy supplying rental housing at reasonable prices by building a complex on the artificial ground above railroad sites. One of the crucial factors to make the artificial ground is the selection of foundation type which can satisfy the given site conditions, such as bearing capacity, construction speed and cost efficiency at the same time. The most representative method to achieve a bearing capacity and construction time is using a micropile. This can be constructed in the narrow space between the railway lines. However, utilization of the micropile entails high cost on overall construction due to the high price of micropile. This is due to, rather than cast-in-place concrete pile or PHC pile which are commonly used for the foundation type on construction sites in Korea. The purpose of this study is to find improvements of the cost efficiency and to find the bearing capacity with the micropile, The Jet Grouting method has been implemented to increase soil strength by making waveform which has a regular bell shape curve to the grout body for reducing the micropile length due to the increase of bearing capacity. The numerical analysis results showed the new micropile achieves higher performance at bearing capacity compared with the existing micropile. Additionally, the factors which should be considered during evaluating the bearing capacity of the new micropile were suggested according to the location and space between the waveform of the grout body.

Keywords: Micropile, Artificial ground, Numerical analysis, Jet grouting, Waveform micropile

1. INTRODUCTION

Artificial ground is widely used for the purpose of securing residential land development in many countries (Lee and Shim, 2004). Recently, the Korean government has also announced a new plan to provide housing for the rapidly increasing population of the capital city. The rental housing will be supplied at a cheaper price than the current market rate using national land such as railroad sites. There are some technicalities that needs to be in construction to build an artificial ground above the railroad site. Especially the type of foundation that has to satisfy the conditions not only needs the bearing capacity relevant to soil characteristics but also railroad conditions. As the railroad is operating during the construction period, the construction method of the foundation has to achieve the construction speed which can minimize the effects to the operating system of railroad. Moreover, it is necessary to consider the narrow space between the railway lines.

[1] PhD Student, Division of Geospace Enginering, Korea University of Science and Technology(UST), 1109 Simindae-Ro Ilsanseo-Gu Goyang-Si South Korea, Tel: 82-31-910-0237, yejang@kict.re.kr
[2] Senior Researcher(Associate professor, UST), Geotechnical Engineering Division, Korea Institute of Construction Technology, 1109 Simindae-Ro Ilsanseo-Gu Goyang-Si South Korea, Tel: 82-31-910-0259, jimmyhan@kict.re.kr
[3] Research Fellow(Professor, UST), Geotechnical Engineering Division, Korea Institute of Construction Technology, 1109 Simindae-Ro Ilsanseo-Gu Goyang-Si South Korea, Tel: 82-31-910-0785, chchoi@kict.re.kr

There is already a list of several types of foundation that fits for railroad sites. Among these methods, micropile is considered as an appropriate method for the foundation of artificial ground above the railroad site. However, micropile generally brings higher construction cost than cast-in-place concrete pile or PHC pile, hence the method to reduce cost without losing bearing capacity has been studied. In order to provide better skin frictional resistance of the piles, a method of installing the micropile at different inclination angles was suggested by researchers. An experiment and numerical analysis result showed that pile inclination contributes to an increase in vertical bearing capacity for both static and seismic loading (Juran et al., 2001; Marwan and Isam, 2004; Tsukada et al., 2006). Choi et al.(2010) and Hong et al.(2012) proposed a pack-micropile using woven geotextile to warp outside of steel and grouting inside of the geotextile in soil layer. Through an experiment, higher frictional resistance was observed as the grouted geotextile obtains better contact between the ground and the pile.

This paper proposes a new concept of micropile for the same purpose to obtain better resistance as shown in the studies listed above. In this study, numerical analysis was performed for the evaluation of the developed micropile based on the new concept of micropile.

2. CONCEPT OF WAVEFORM MICROPILE

Soil jet grouting method is adapted for a new concept of micropile. Soil strength is increased once combined with grouting mortar and soil while digging in the ground. But one difference with the existing soil jet grouting method is forming a waveform to the grout body with certain pressure.

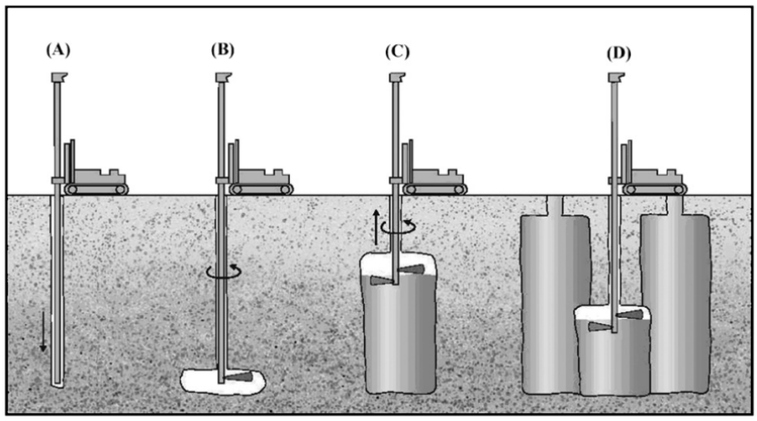

Figure 1. Sequence of jet grouting method (Nikbakhtan and Osanloo, 2009)
(a) Drilling, (b) Jetting test, (c) jetting forming a column, and (d) completion

Figure 2 shows the concept of micropile with the waveform grout body. The size of waveform must be determined after considering soil condition as shown in Figure 2 (a) S=0(no space between bumps) and (b) S>0(space between bumps). The size of the bump is a main factor developing bearing capacity of pile according length and space. Higher performance is expected at bearing capacity compared with the existing micropile. For example, if the space between bumps is less than or equal to zero, the skin friction of micropile will be presented as Figure 2(a). On the other hand, if the space in between bumps is larger than zero, the pile will be supported by skin friction and side friction together as shown in the Figure 2(b). Since the size of the bump is critical, the effect of the location of the bump was analyzed using numerical method in this study.

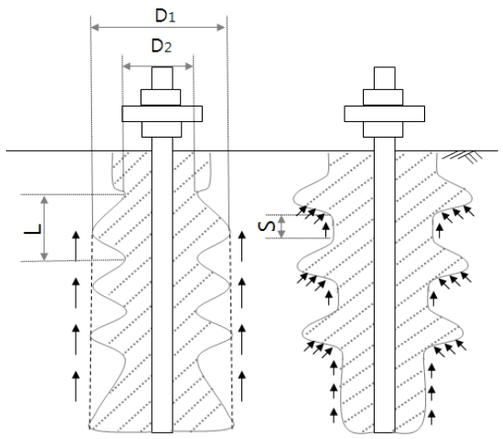

(a) S=0 (b) S>0

Figure 2. Concept of waveform micropile

3. ANALYSIS MODEL

3.1 Soil and foundation model

Figure 3 presents a soil profile of expected construction site in Korea with N-values along the soil depth. N-values were found to range from 9 to 50, indicating various soil types for weak soil, weathered soil, weathered rock and soft soil.

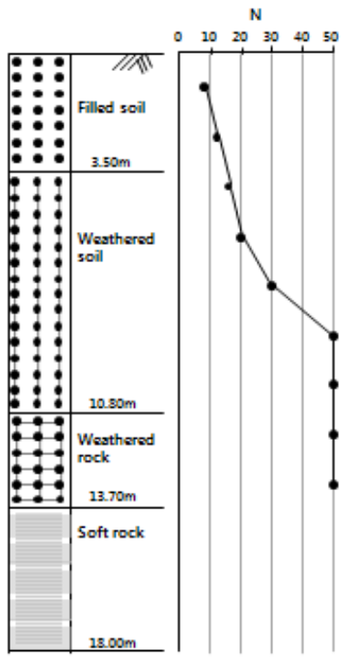

Figure 3. Boring log of study site

Analysis models were established from model A to C to compare bearing capacity with different shapes of micropile. Each analysis model shows a certain type of grouting applied; (a)

General type of micropile, (b) Micropile with soil jet grouting (without waveform), (c) Micropile with soil jet grouting (with waveform). Models for the general type of micropile without waveform have been used to figure out the effect of the waveform micropile. Especially the location and space between the waveform of the grout body was considered as a significant factor achieving improvements of bearing capacity. Thus, the waveform micropile was categorized into several models to attain various results according to different shapes of the grout body.

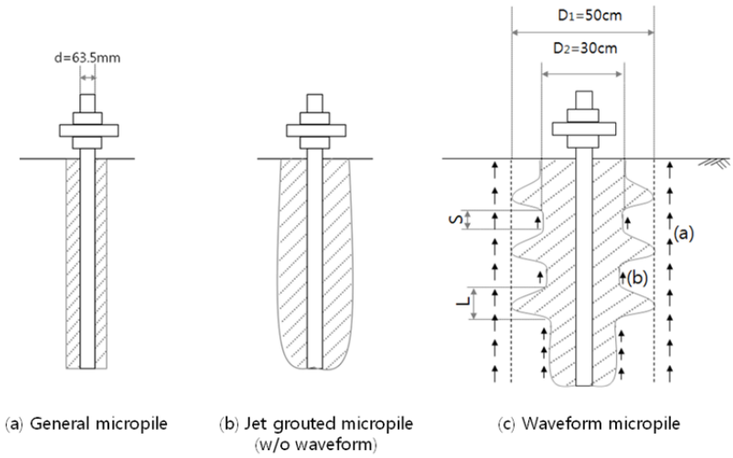

Figure 4. Analysis model for vertical bearing capacity

The analysis models have been prepared according to the previous description as shown in the table below. The presented cases C1, C2, C3 and C4 were used to analyze static bearing capacity of the pile, while C1, C5, C6 and C7 models were used to analyze bearing capacity for lateral load and seismic loading.

Table 1. Pile dimension and grout strength

Analysis type			
C1	General micropile D=180mm(fck*=30MPa), Length=16m	C5	Micropile with soil jet grouting D_1=D_2=300mm, Length=13.7m
C2	Micropile with soil jet grouting D_1=D_2=500mm, Length=13.7m		
Waveform micropile D_1=500, D_2=300mm, Length=13.7m			
C3	L&S=0.5m	C6	L=1m, S=0
C4	L:0.5m, S:2.5m	C7	L&S=1m

3.2 Evaluation of bearing capacity

In this study, two types of analysis have been performed on the static and dynamic bearing capacity. To analyze FEM (finite element method) Plaxis version 8.0 and OpenSees were utilized for the static and dynamic analysis respectively. Figure 5(a) describes element meshes and the pile modeling for static analysis consisted of triangular elements with fifteen nodes on the axis-symmetry condition. Figure 5(b) conceptualizes the interaction between pile and soil that has

been fulfilled for the dynamic analysis. With the purpose of evaluating the lateral bearing capacity under the seismic loadings, the p-y curve was used to describe the pile-soil interaction along with the depth.

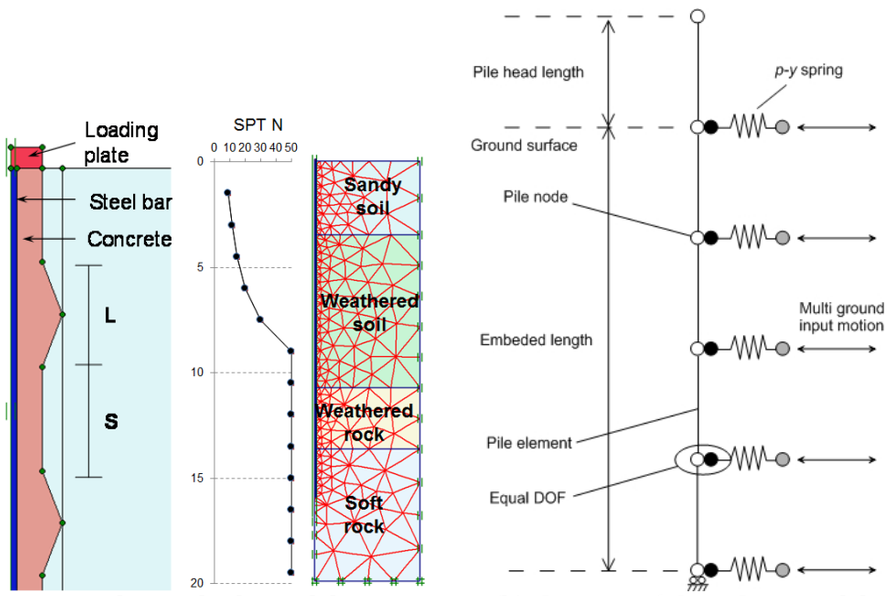

(a) Element meshes and pile modeling (b) Concept of OpenSees model

Figure 5. Concept of FEM analysis

Many researchers studied how to determine the pile-soil interaction. The p-y curve which was developed by Matlock(1970), Reese et al.(1974) and the marine structure design standard(API, 2007; DNV, 2010 and etc.), is regarded as the acceptable method of laterally loaded piles. The research to find a suitable method to be performed on the static and dynamic issues is ongoing. For the analysis in this paper, the p-y curve was also used to evaluate dynamic bearing capacity of waveform micropile. Yoo et al.(2013) suggested the dynamic p-y curve through centrifuge test and numerical analysis which is shown in table 2.

Table 2. Dynamic p-y curve (Yoo et al., 2013)

Dynamic p-y curve	$p = \frac{y}{\frac{1}{k_{ini}} + \frac{y}{p}}$	$p = \frac{Kp_u}{p_u + K\frac{D}{100}}$
	Initial k (N/cm^2)	Ultimate soil reaction$((N/cm)$
Loose Sand	$K = 4.26DP_a\left(\frac{\sigma'}{P_a}\right)^{0.5}$	$p_u = 12.5DK_p\gamma' z^{1.02}$
Dense Sand	$K = 7.29DP_a\left(\frac{\sigma'}{P_a}\right)^{0.5}$	$p_u = 13.3DK_p\gamma' z^{0.90}$

Where, p_u: ultimate soil reaction, k_{ini}: initial subgrade reaction modulus, K: subgrade reaction modulus, P_a: atmospheric pressure, K_p: coefficient of Rankine's passive earth pressure, D: pile diameter and z: soil depth.

Seismic loadings have been prepared with the Hachinohe earthquake which has peak acceleration of 0.154g corresponding seismic design standard of Korea.

4. ANALYSIS RESULT

In this chapter the analysis results are shown from static and dynamic analysis. Vertical and lateral behavior are included in the static analysis result, while seismic behaviors are shown in the dynamic analysis result.

4.1 Static analysis

Figure 6 shows a comparison of load-movement curves for the general micropile, the jet grouted micropile and the waveform micropile subjected to axial compression loading condition at the pile head. Axial load increases until the movement of pile reaches to about 30~40mm. The ultimate load was estimated in order of test cases according to C2, C3, C4 and C1 with the values 3,720kN, 2,450kN, 2450kN and 2,310kN, respectively. It is interesting to note that ultimate load of C3 and C4 corresponded closely regardless of the bump. But a closer look at the figure indicates that the displacement of C3 is less than the displacement of C4 under the same loading condition. C3 also achieved considerable decreases of displacement at about 40% compared to general micropile C1 under the design load 1,000kN. In conclusion, the waveform micropile provides higher bearing capacity.

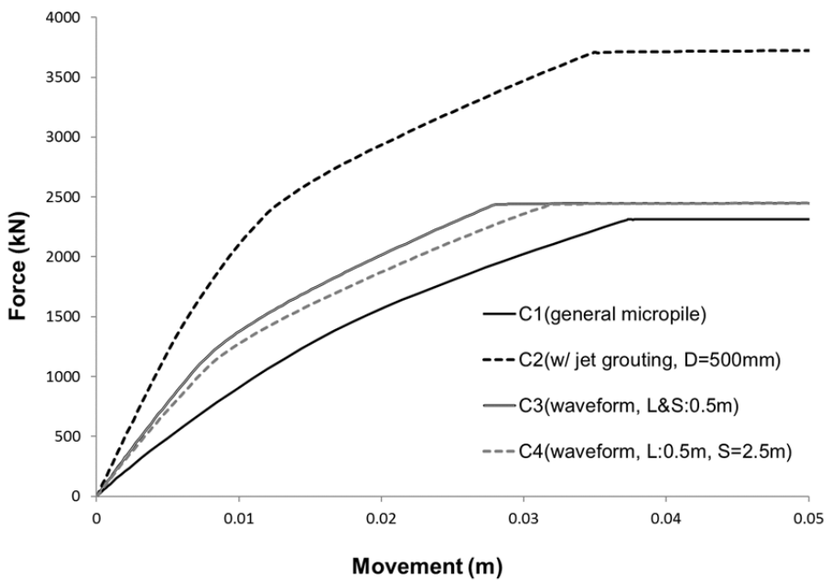

Figure 6. Pile head load-movement curves of micropile

Table 3 presents the summary of the pile head movement at allowable material strength. The value of C3 shows a higher resistance at about 35% than C1 in spite of the pile length was decreased about 15% (2.3m). Especially the waveform micropile shows a trend as the space and length of the bump varies. For example, the displacement was decreased at about 4.3% as the

length of the bump increased to double (from $1D_1$ to $2D_1$) at the same space of bump. On the other hand, the displacement shows lesser values when the space of bump was decreased (from $5D_1$ to $1D_1$) with the same length of the bump. Based on this observation, it is expected that the bearing capacity of waveform micropile will be shown higher performance as the length increases and space decreases.

Table 3 Pile head movement at allowable material strength

Case	C1	C2	C3	C4
Pile head movement(mm)	17.9	8.2	11.7	13.4

The load transfer curve obtained for both the general micropile and the waveform micropile under the 10mm of pile head was displaced as shown in figure 7. The results of the jet grouted micropiles indicate that the waveform was contributed to increase at the soil depth of 0~3.5m where the ground condition was soft. But, as the ground changes from soft to stiff, along with the soil depth, only a small increase was detected in skin friction. This fact reveals that the waveform of micropile contributes to better achievement of skin friction when the ground is relatively soft.

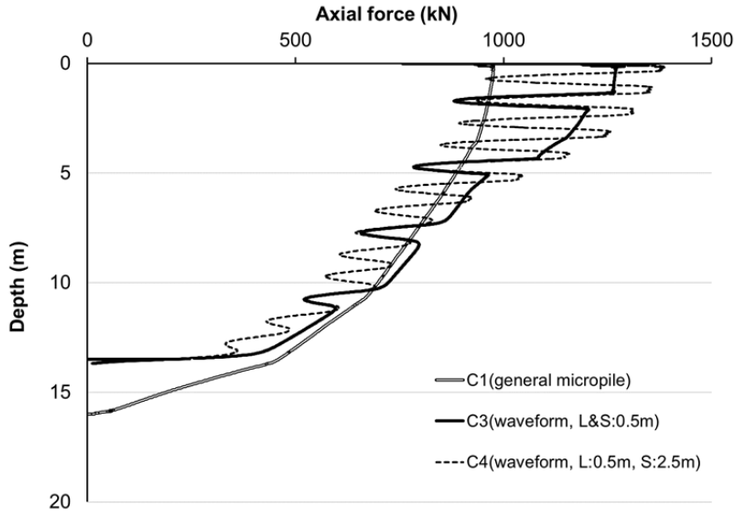

Figure 7. Comparison of axial load transfer curves of micropiles
(Pile head displacement = 10mm)

Figure 8 shows the analysis result of curves; (a) Lateral displacement (b) moment along the pile depth when 30kN was applied at the pile head. The maximum lateral displacement of 0.216m was estimated at the general micropile C1, and decreased to 0.088m for jet grouted pile C5 and reached 0.079m, 0.080m for the waveform micropile C6, C7, respectively. The decrement of lateral displacement at C5 was about 60% less than C1. However, there was only a small decrement for waveform micropile model (C6, C7) compared to the jet grouted micropile (C5) which was about 10%. The result indicates that the performance of laterally loaded waveform micropile was not contributed due to mobilizing higher capacity under the lateral static load.

In the case of moment analysis, the maximum moment was estimated of 51.1kN·m for the general micropile(C1) and decreased to 46.3~46.5 kN·m for the waveform micropile. The waveform micropile decreased about 10% compared to the general micropile due to the shapes of analysis cases being different. Thus, the compressive stress was estimated for the reasonable comparison with the result. Maximum compressive stress for C1 and C5 was 89.2MPa and

17.5MPa respectively, while the waveform micropile showed 3.8MPa. Estimated compressive stress at the waveform micropile was about 96% less than general micropile. In conclusion, the waveform micropile was developing higher static bearing capacity than the general micropile and the jet grouted micropile.

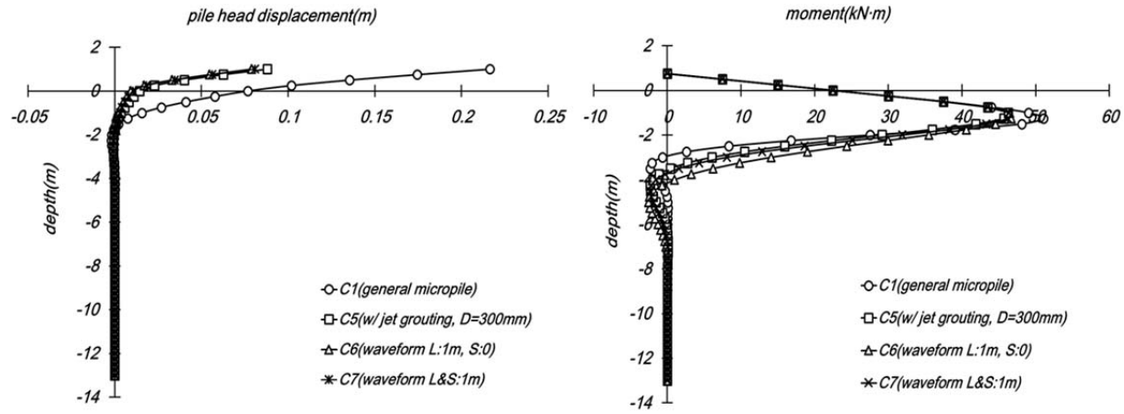

(a) Lateral displacement vs. depth (b) Moment vs. depth

Figure 8. Behavior of laterally loaded micropiles

4.2 Dynamic analysis

The analysis result of the lateral displacement along the pile depth subjected to seismic loads is shown in figure 9. In the general micropile (C1), the largest lateral displacement of the pile head was 0.208m, while the waveform micropile C6(L:1m, S:0m) and C7(L1m, S:1m) measured 0.072m and 0.084m respectively. In comparison to the general micropile, the lateral displacement of the jet grouted micropile decreased to approximately 51%. Moreover, within the jet grouted micropile, the lateral displacement of the waveform micropile decreased to 29%, compared to the one of the jet grouted micropile without micropile. For all cases, the piles with waveform appeared to be highly resistant to lateral loads.

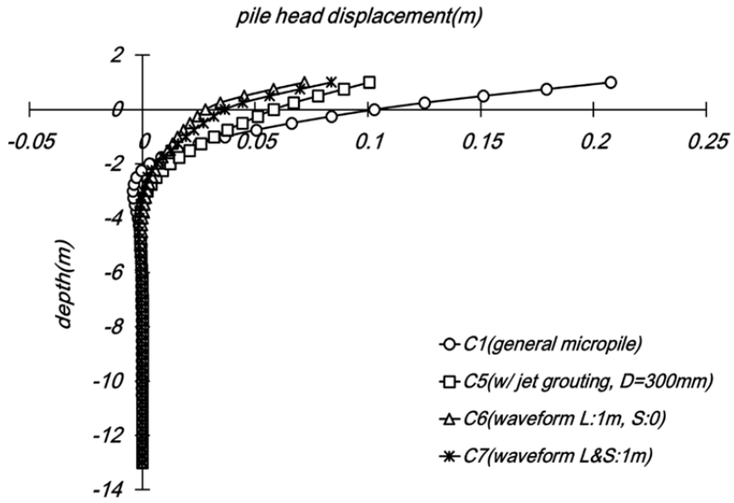

Figure 9. Lateral displacement along the pile depth

Below is the analysis result of lateral displacement along the pile depth subjected to seismic loads. Figure 10 shows the lateral displacement-time history for each model at ground surface. Just like the results for maximum lateral displacement of pile head, regardless of seismic loads, the maximum value turned up the highest for general micropile, while lateral displacement of the waveform micropile appeared to be the lowest among all the other models. When the Hachinohe earthquake was applied, most significant change was observed in the general micropile compared to other models. This is because lateral stiffness of general micropile is lowest which leads to an increase in natural frequency.

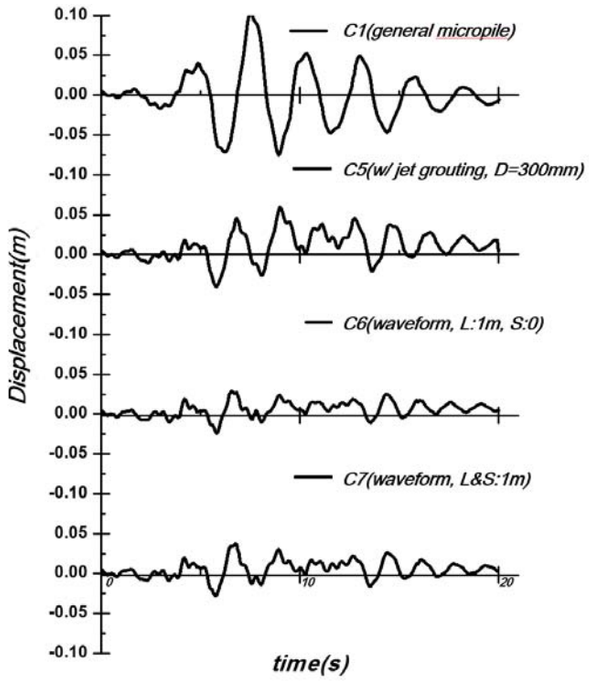

Figure 10. Displacement-time history at seabed

4. CONCLUSION

In this study, the numerical analysis method was used to analyze the static and the dynamic bearing capacity of the waveform micropile. Several analyses have been performed to analyze the characteristics of affecting factors. As a result, these conclusions were drawn;

i) Waveform micropile decreased in axial movement to about 40% compared to the general micropile under the design load. This indicates that the waveform micropile provides higher bearing capacity.
ii) The skin friction of the waveform micropile varies according to soil strength. Based on this observation, it is concluded that further study is required to investigate the effects of diverse soil condition.
iii) Space and length of the bump is considered as key factors to achieve higher bearing capacity for both static and dynamic analysis. It is expected that the bearing capacity of waveform micropile will show higher performance as the length increase and space decreases.

ACKNOWLEDGEMENT

This research was supported by a grant from “Design and construction of artificial ground with the vertical spaces above existing urban infrastructure” which is funded by The Korea Institute of Construction Technology.

REFERENCES

- API RP 2A-WSD. (2000). *Recommended practice for planning, designing and constructing fixed offshore platforms-working stress design*, API RP 2A-WSD, 21st edition.
- Choi, C., Cho, S.D. (2010). Field verification study for micropile load capacity, *Proc. of 10th ISM Workshop*, 1-10 p.
- DNV. (2010). Design of Offshore Wind Turbine Structures, DNV-OS-J101, Oslo. Norway, 125-127 p.
- Germanischer Lloyd (GL). (2005), *Rules and guidelines industrial services IV. 2. guideline for the certification of offshore wind turbines*, Hamberg, Germany.
- Hong, W. P., Cho, S. D., Choi, C., and Lee, C. M. (2012). Skin friction mobilized on pack micropiles subjected to uplift force, *Journal of Korea Geotechnical Society*, Vol 28, No. 6, 19-29 p.
- Juran, I., Benslimane, A., and Hanna., S. (2001). Engineering analysis of dynamic behavior of micropile systems, Transportation Research Record No. 1772. Soil Mech 2001, 91–106 p.
- Lee, C. M., and Shim, J. H. (2004). A case study on a classified by characteristics of pedestrian deck, *Journal of Architectural Institute of Korea*, Vol. 24, No. 2, 559-562 p.
- Marwan, S., and Isam, S. (2004). Three-dimensional finite element analysis of the seismic behavior of inclined micropiles, *Soil Dynamics and Earthquake Engineering*, Vol. 24, No. 6, 473-485 p.
- Matlock, H. (1970), Correlations for Design of Laterally Loaded Piles in Soft Clay. *Proc. 2th Offshore Technology Conference*, Houston. Texas., Vol. 1, 577-607 p.
- Nikbakhtan, B., and Osanloo, M. (2009). Effect of grout pressure and grout flow on soil physical and mechanical properties in jet grouting operations, *Journal of Rock Mechanics and Mining Sciences*, Vol. 46, No. 3, 498-505 p.
- Reese, L. C., Cox, W. R., and Koop, F. D. (1974), Analysis of Laterally Loaded Piles in Sand, *Proc. 6th Offshore Technology Conference*, Houston. Texas., Vol. 2, 473-483p.
- Tsukada, K., Miura, Y., Tsubokawa, Y., and Otani., G. L. (2006). Mechanism of bearing capacity of spread footings reinforced with micropiles, *Journal of soils and foundations*, Vol. 46, No. 3, 367-376 p.
- Yoo, M.T., Choi, J.I., Han, J.T., and Kim, M.M. (2013). Dynamic p-y Curves for Dry Sand by Dynamic Centrifuge Tests, *Journal of Earthquake Engineering*, Vol. 17, No. 7, 1082-1102 p.